applied optics

Optimization of a lightweight mirror with reduced sensitivity to the mount location

PING JIANG[1,†] AND PINGWEI ZHOU[1,2,*,†]

[1]Changchun Institute of Optics, Fine Mechanics and Physics, Chinese Academy of Sciences, Dong-Nanhu Road 3888, Changchun 130033, China
[2]University of Chinese Academy of Sciences, Beijing 100039, China
*Corresponding author: npuzhoupw@163.com

Received 20 November 2019; revised 18 March 2020; accepted 18 March 2020; posted 19 March 2020 (Doc. ID 383391); published 20 April 2020

Due to optical performance requirements, the primary mirror assembly must be unaffected by environmental influences. These environmental influences include gravity, axial assembly error, flatness error of mounting interface, and thermal change, which can degrade the mirror surface's accuracy. The flexure mounts can be used to isolate the load transfers to the mirror in case of a flatness error and thermal change. The mirror surface's accuracy will degenerate significantly when the flexure mounts have deviations from the optimum axial mount location due to mirror fabrication and a testing error at the center of gravity. These two error terms introduce an accuracy of mount locations on the order of millimeters. In this paper, we describe a method to reduce the sensitivity of a lightweight mirror to the mount location. First, we introduce a design criterion that determines the sensitivity. Then, the topology and parametric optimization are used to specify selective reinforcement of the mirror structure in which the design criterion is taken as the objective function. With our method, the lightweight ratio of a 2 m mirror has been improved from 86.8% to 88.5%, and its sensitivity to the mount location has been reduced from 1 nm/ ± 1 mm to 0.6 nm/ ± 1 mm.

https://doi.org/10.1364/AO.383391

1. INTRODUCTION

Astronomical and earth observations performed using space telescopes have become increasingly common in recent years. To increase the collecting power and improve the angular resolution, larger aperture primary mirrors are needed [1]. The primary mirror is the heaviest component in the telescope and it needs to be lightweight. The goal of primary mirror design is to satisfy the requirements of mirror surface accuracy and location, which are obtained by optical error analysis and technical specifications. When designing the primary mirror assembly, these requirements should be taken as objectives or constraints. The requirement of mirror surface accuracy refers to the ability to be unaffected by environmental influences. These environmental influences include gravity, the axial assembly error, the flatness error of the mounting interface and thermal change, under which the mirror surface accuracy is degraded. The requirement of location can be further divided static location and dynamic location. The static and dynamic locations are related to the mass, compliance of support and fundamental frequency, respectively. The above-mentioned requirements can be directly quantified through finite element analysis and testing. While low distortions are necessary, an important additional criterion is that designs are tolerant to imperfect positioning of the mounts relative to the optimum axial mount location. Up until now to the best of our knowledge, no quantification of this criterion has been proposed.

To reduce the cost of the launch into space, it is important decrease the weight of the primary mirror during the design process. Different design methods for lightweight mirrors have been reported, which include the use of high-performance materials or new lightweight structures. Among them, topology optimization is widely used as it can break through the limits of the existing structure. The topology optimization of the primary mirror of a multispectral camera under self-weight and polishing pressure was presented by Park *et al.* [2,3]. During the topology optimization, the Strehl ratio and mass were taken as the objective and constraint, respectively. After optimization, the primary mirror had good optical performance with low mechanical deflection. To minimize the mass and optical aberrations [4], structural optimization of a 1.2 m diameter Zerodur space mirror was carried out by Sahu [4]. However, the milling process, which is typical in fabrication of open-back mirrors, was not feasible to get the desired design result. A lightweight design for a Zerodur primary mirror with an outer diameter of 566 mm was studied by Chen *et al.* [5], in which deformation under polishing pressure, and vertical-axis gravity and horizontal-axis gravity are considered. After optimization, the needed lightweight ratio, optical performance, and stiffness were well achieved. Liu *et al.* also created a lightweight design for a large-aperture primary mirror by using topology optimization [6]. Its design goal is to maximize the stiffness of mirror, which equates to the minimum of structural compliance. In addition, the topology and the parametric optimization-based lightweight design of a space reflective mirror was studied by Liu *et al.* [7]. In this reference, the value of the root mean square (RMS) of surface accuracy and the fundamental frequency were taken as the objective merit function and constraint, respectively. The optimization result shows that the lightweight rate, optical performance, and stiffness have been improved when compared to the initial design.

As mentioned above, excellent work has been done and different design criterions have been taken as an objective function. However, satisfying the traditional design requirements is not enough to obtain good performance in practice. It is common knowledge that the mirror surface accuracy will degenerate significantly when the flexure mounts have deviations from the optimum axial mount location due to mirror fabrication and the testing error of the center of gravity. The fabrication of the SiC mirror adopts the process, which is like the casting process in which a fabrication error can achieve 1 mm. Fabrication errors will change the mass distribution, which determines the neutral surface. Because the neutral surface cannot be directly tested, the practical axial assembly location is determined by testing the center of gravity. These two error terms introduce an accuracy of mount locations on the order of millimeters. When the designed mirror is too sensitive to the mount location, the tested surface accuracy under gravity may exceed the design requirement. When the deviation is too large to be acceptable, a new set of flexures should be made to compensate for the mirror's fabrication errors. This procedure is, however, time-consuming and costly [8,9] Therefore, it is important to reduce the sensitivity to the mount location at the stage of structural design [10,11].

From the above analysis, we can see that reducing the sensitivity to the axial mount location is critical to achieving low surface distortions in practice. However, the quantitative relation between the sensitivity and mirror design has not been studied. In this paper, a design criterion that determines the sensitivity is introduced. Then, the topology and parametric optimization are used to specify selective reinforcement of the mirror structure in which the design criterion is taken as the objective function. The effectiveness of the proposed design criterion has been verified.

2. PERFORMANCE METRICS

Typically, space mirrors are fabricated and tested on the ground, and then launched into space. The mirror surface accuracy in orbit may be degraded by gravity relief and thermal change. To fully verify the optical performance of space telescopes on the ground, it is necessary that the mirror surface accuracy is maintained with high precision. In addition, to prevent the mirror from vibration damage during the launch, it is very important to ensure its good dynamic stiffness.

To ensure the high surface accuracy of the mirror, the surface accuracy degradation caused by the disturbance of gravity, thermal change, the flatness error of the mounting surface and axial mount accuracy are considered in the design process of the space mirror assembly. The comprehensive surface accuracy index is decomposed into independent indexes according to the disturbance type. In this way, the comprehensive surface accuracy index can be satisfied when each sub-index separately meets the requirements.

For the present study, a 2 m SiC primary mirror with three-point supports is designed. According to the optical error analysis, the required comprehensive surface accuracy should not exceed 7.8 nm [12]. Then, 7.8 nm is decomposed into 5.2 nm for gravity, in which the distortion of single mirror is less than 4.5 nm, and that of support is not more than 2 nm. The surface distortion caused by the assembly error is less than 5.5 nm, which mainly refers to the surface distortions induced by a 0.1 mm flatness error of the mounting face. When the temperature change is 4°C, the allowed degradation of surface accuracy is 2 nm, as shown in Fig. 1.

Furthermore, the performance of the primary mirror is related to the assembly precision. When the flexure is located at the mirror's neutral surface [12], the surface distortion due to gravity can be minimized. And, the mirror surface accuracy will degenerate significantly when the flexure mounts have deviations from the optimum axial mount location due to mirror fabrication and the testing error of the center of gravity. Therefore, to achieve good performance in practice, the sensitivity to the mount locations is taken as a design index.

The traditional design process for a lightweight mirror is shown in Fig. 2. In accordance with this process, a 2 m lightweight primary mirror assembly has been designed and fabricated by our team. When designing the 2 m primary mirror, topology optimization was used, in which the design objective and constraint is the rigidity and mass, respectively. After optimization, the mass was 265 kg, and the lightweight rate reached 86.8%. When supported at an optimum axial mount location, the surface accuracy under self-weight is 4.61 nm. The specific design index is listed in Table 1. From Table 1, it can be concluded that every single design index has been meet.

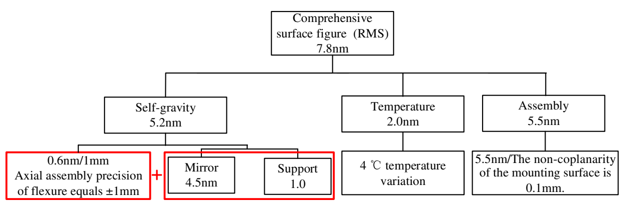

Fig. 1. Schematically illustrates the performance metrics.

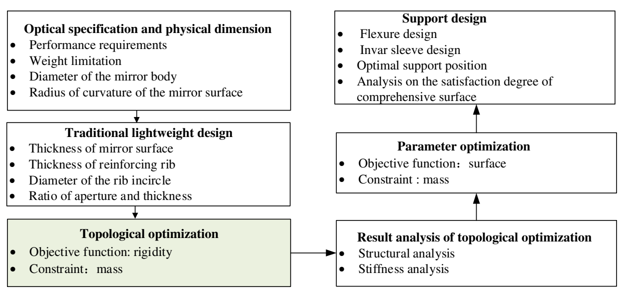

Fig. 2. Traditional design process of lightweight mirror.

Table 1. Design Results of Different Design Indices

Design Index	Result	Allowed Value
1 g gravity	4.61 nm	5.2 nm
4°C thermal change	1.38 nm	2.0 nm
Forced displacement of 0.1 mm	5.29 nm	5.5 nm
Fundamental frequency	130 Hz	100 Hz

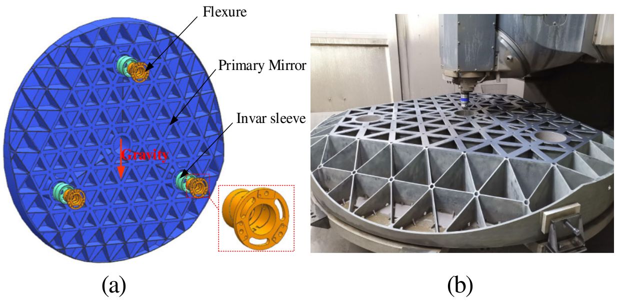

Fig. 3. (a) Exploded view of predesigned lightweight primary mirror assembly showing the symmetries, invar sleeve, gravity orientation, and illustration of the adopted flexure configuration [12]. (b) The 2 m primary mirror under milling.

The exploded view of the predesigned 2 m lightweight primary mirror is shown in Fig. 3(a). The fabricated 2 m primary mirror under milling is shown in Fig. 3(b). The milling process is expected to completed by April 2020.

The sensitivity of the predesigned 2 m primary mirror to the mount locations is shown in Fig. 4. The sensitivity is 1 nm/ ± 1 mm, which means that the degradation is 1 nm when the deviation from the optimum axial mount location equals 1 mm. As the axial assembly precision is 1 mm, the surface accuracy induced by gravity can be calculated at 5.6 nm, which exceeds the design index (5.2 nm). As shown in Fig. 1, the allowable sensitivity to the mount locations is 0.6 nm/ ± 1 mm. So, the 2 m primary mirror needs further design improvement.

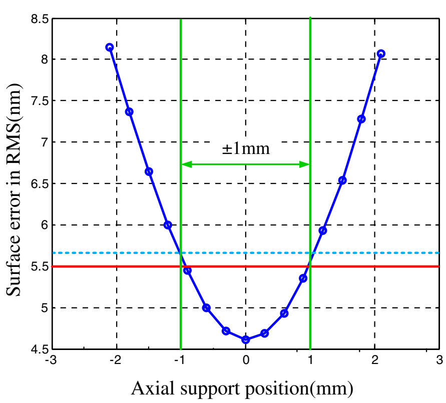

Fig. 4. Sensitivity curve showing the optimal surface accuracy (4.61 nm), axial assembly accuracy (green line), and the allowed value under gravity (red line).

3. SENSITIVITY OF SURFACE DISTORTION TO AXIAL MOUNT LOCATIONs

For testing and aligning large space optical systems, it is convenient when the mirror's optical axis is perpendicular to the gravity direction. Ground testing with their optical axes in a horizontal position can result in less distortion than in a vertical orientation. Figure 5 shows the distribution of the support force and moment applied for the three-fold axisymmetric mirror. In this paper, each flexure is designed to take a third of the mirror's weight. In the case of the gravity vector acting normal to the axis of symmetry, we can obtain

$$\begin{cases} F_{X1} = F_{X2} = F_{X3} = \frac{m \cdot g}{3} \\ F_{Z1} + F_{Z2} + F_{Z3} = 0 \\ \frac{2 \cdot F_{Z1} \cdot h}{3} + \frac{F_{Z2} \cdot h}{3} + \frac{F_{Z3} \cdot h}{3} + M_{Y1} + M_{Y2} + M_{Y3} = m \cdot g \cdot \epsilon_1 \, , \\ F_{Z2} = F_{Z3} \\ M_{Y1} = M_{Y2} = M_{Y3} \end{cases} \quad (1)$$

where F_{Xi} is the force balancing the gravity, F_{Zi} is the axial force, and M_{Yi} is the moment about Y axis in which the value of i is 1 to 3. ϵ_1 is the distance from axial position of flexure to the mirror's center of gravity.

Then we can get

$$\begin{cases} F_{Z1} \cdot h + 3M_{Y1} = m \cdot g \cdot \epsilon_1 \\ F_{Z1} = -2F_{Z2} = -2F_{Z3} \end{cases} . \quad (2)$$

Inertia relief is an advanced option in ANSYS that allows you to simulate unconstrained structures in a static analysis. It gets the FEA model to exactly balance the force difference (applied force minus weight) in a static analysis with acceleration body forces over the whole structure so that the reaction on the constraint is zero. During analysis, enough constraints are required to prevent free body translation and rotation [six for a three-dimensional (3D) structure]. In this paper, inertia relief is used to analyze the surface distortion under self-weight at different mount locations. By using inertia relief, we can study how each load given in Eq. (1) affects the surface distortions. The primary mirror without flexures is to be analyzed as a free–free structure. First, three mass points are established at the centers of the three support holes and with different axial locations. Second, to distribute the external load applied at mass points to the mirror, the RBE3 elements are created to connect the mass points to the nodes on the bonding interface, respectively.

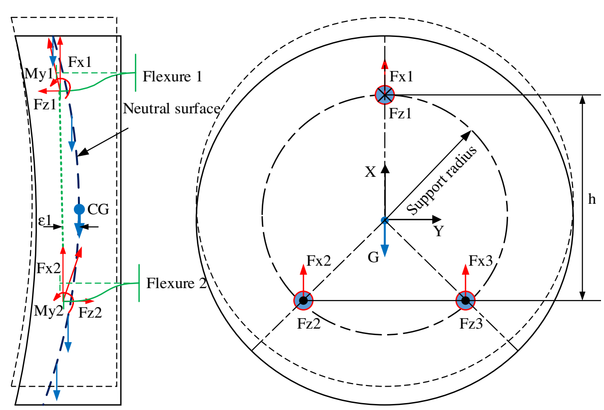

Fig. 5. Schematic distribution of the support force and moment.

The RBE3 element is the flexible connecting element used to distribute loads without introducing additional stiffness of structures. Third, the force balancing the gravity, the unit axial force, and the unit moment about the y axis are applied to the mass points, respectively. Last, three arbitrary nodes apart from the nodes on the bonding interface can be selected as constraint points, in which x degree of freedom is prevented at three nodes, y degree of freedom at two nodes, and z degree of freedom at one node. After each analysis, both the force reaction and moment reaction have been calculated to make sure they are virtually zero. Figure 6 shows the surface distortion in which the piston and tilt are removed. Figure 6(a) shows the surface distortion as an example when $F_{X1} = F_{X2} = F_{X3} = \frac{mg}{3}$ is applied at the three mass points with the same axial position of center of gravity. When $F_{X1} = F_{X2} = F_{X3} = \frac{mg}{3}$ is applied at different axial locations, the resulting moment causes different the surface distortion δ_G accordingly.

In previous research [12], the surface distortions δ_A and δ_M, as shown in Figs. 6(b) and 6(c), were used to compensate each of the surface distortions with a different axial position. As shown in Fig. 6(b), the surface distortion δ_A is astigmatic. The residual surface distortion δ_{Rout}, which presents the uncorrected distortion and the optimal axial force $F_{z1}(17.5N)$, remains constant. The residual surface distortion and the result obtained from the primary mirror assembly FEA model, including flexure when supported at the optimum position, are shown in Fig. 7.

The fact that the optimal axial force remains constant indicates that the surface distortion δ_G at different mount locations contains a constant astigmatic aberration. The reason for the constant astigmatic has been explained in our previous research [12]. As discussed, the minimum surface distortion can be obtained when the constant astigmatism is completely corrected. For the predesigned mirror assembly shown in Fig. 3, the astigmatic error would be corrected completely when the axial force F_{Z1} equals 17.5N. Specifically, the optimal axial force is the inherent attribute, which depends on the mirror's structure.

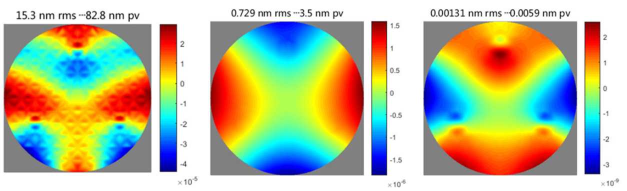

Fig. 6. Surface distortion analysis by inertia relief. (a) $F_{X1} = F_{X2} = F_{X3} = \frac{mg}{3}$, (b) $F_{Z1} = 1N$, $F_{Z2} = F_{Z3} = -0.5N$, and (c) $M_{Y1} = M_{Y2} = M_{Y3} = 1\mathrm{N} \cdot \mathrm{mm}$.

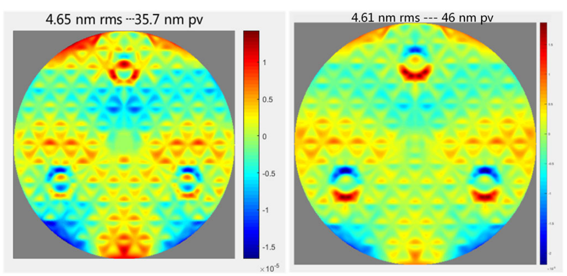

Fig. 7. (a) Residual surface distortion. (b) Surface distortion when supported at optimum mount position.

For a given flexure, the value of M_{Y1} depends on the flexure's bending stiffness and the supported mirror's weight.

When the axial force moves away from the ideal axial force, the uncorrected astigmatic error can be calculated as

$$(F_{z1} - F) \cdot \delta_A. \tag{3}$$

The surface distortion due to the deviation from the needed moment is given by

$$\left(M_{Y1} - \frac{m \cdot g \cdot \epsilon_1 - F \cdot h}{3}\right) \cdot \delta_M = \frac{(F_{z1} - F) \cdot h}{3} \cdot \delta_M. \tag{4}$$

The terms of optical distortion are mostly uncorrelated. The RMS surface distortion at an arbitrary mount location can be summed by the root sum of squares method,

$$\delta_{\mathrm{RMS}} = \sqrt{(F_{z1} - F)^2 \cdot \delta_A^2 + \frac{(F_{z1} - F)^2}{9} \cdot h^2 \delta_M^2 + \delta_{Rout}^2}. \tag{5}$$

Then, the equation can be transformed into the conic form, so

$$\frac{\delta_{\mathrm{RMS}}^2}{\delta_{Rout}^2} - \frac{(F_{z1} - F)^2}{\frac{\delta_{Rout}^2}{\delta_A^2 + \frac{h^2 \delta_M^2}{9}}} = 1. \tag{6}$$

The eccentricity reflects the opening size of the hyperbola curve and can be calculated as

$$e = \sqrt{\frac{\delta_{Rout}^2 + \frac{\delta_{Rout}^2}{\delta_A^2 + \frac{h^2 \delta_M^2}{9}}}{\delta_{Rout}^2}} = \sqrt{1 + \frac{1}{\delta_A^2 + \frac{h^2 \delta_M^2}{9}}}. \tag{7}$$

It is known that the larger the eccentricity is, the larger the opening size is, and the sensitivity curve with a larger opening size is smoother, which means that the mirror is less sensitive to the mount location. So, the eccentricity and the lowest point of the sensitivity curve are taken as the objective function and the mirror mass as the constraint in the topology optimization. The equation of the hyperbola can be expressed as

$$y^2/a^2 - x^2/b^2 = 1 \ (y > 0). \tag{8}$$

Due to the error budget shown in Fig. 1, the RMS of 1 g gravity should be less than 4.5 nm, and the sensitivity is 0.6 nm/ $\pm$ 1 mm. Based on Eq. (8), when x equals 0 and ± 1, y should be 4.5 and 5.1. Then, $a^2 = 20.25$, $b^2 = 4.34$, and the eccentricity $e = 1 + b^2/a^2$ equals 1.21.

To achieve the sensitivity requirement, the eccentricity of the sensitivity curve must satisfy

$$e = \sqrt{1 + \frac{1}{\delta_A^2 + \frac{h^2 \delta_M^2}{9}}} \geq 1.21. \tag{9}$$

The detailed three-step design process for a new 2 m primary mirror is shown in Fig. 8. The steps are: the traditional lightweight design, the topology optimization for sensitivity and self-weight surface distortion, and the result analysis of the topology optimization.

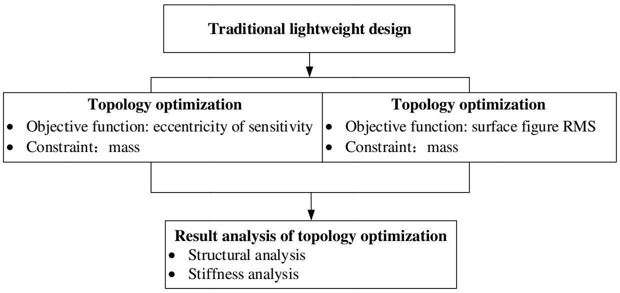

Fig. 8. Detailed design process for a new 2 m primary mirror.

4. LIGHTWEIGHT DESIGN OF THE 2M MIRROR

A. Traditional Design of the Mirror

For the present study, a partially closed back monolithic, 2 m SiC primary mirror configuration is examined. The mirror is supported by three supporting holes located on its back. The supporting radius is 0.68 m, the depth is 0.18 m, and the thickness of the front panel is 5 mm. These structural sizes are determined by empirical equations. The triangular [13,14] isogrid pattern has a 0.08 m inscribed circle diameter. For fabrication simplicity and better thermal performance, the mirror is usually designed as a centrally symmetric structure, and the lightweight ribs distributed on the back of the mirror have a distinct geometric distribution. Due to the fabrication limit of our optical shop, the initial thicknesses of the ribs are set to 4 mm. The mass of the initial mirror is 237 kg and an 88.3% lightweight ratio was achieved. The 2 m primary mirror after the initial design is shown in Fig. 9, and the detailed geometric parameters and mass characteristics of the mirror are listed in Table 2.

B. Topology Optimization of the Mirror

According to the idea of continuum structure topology optimization, the finite-element model is established with a hexahedron mesh [15,16]. A description factor, ρ, is introduced for each element. Whether there is material in each element or not is determined by a ρ value of 1 or 0. In addition, intermediate density values are penalized by a penalty factor, and the intermediate density values are then clustered at both ends of the 0 to 1 range, so that the topology optimization model of the continuous variable can converge well to the optimization model.

The data flow of topology optimization in which RMS is taken as the objective function is shown in Fig. 10. First, the responses (Dresp1 card) of the displacement of nodes located on the mirror surface are built in the finite element preprocessor HyperMesh. And the mass response is also built and set as constraint. Second, the responses of displacements are composed into the Dresp3 card, which defines the parameters to be transferred to an external function. Third, the RMS calculation script (external function) is built in HyperMath. Then the nodal displacements are passed to the HyperMath script and the calculated RMS from the script is used as an optimization objective. The load steps are built just like that discussed in Section 3.

Figure 10(a) shows the material distribution results obtained by the first topology optimization in which the surface distortion RMS and the mass are used as the topology objective and the constraint. Meanwhile, Fig. 10(b) shows the material distribution results obtained by the second topology optimization in which the eccentricity and the mass are used as the topology objective and the constraint. The red part represents elements

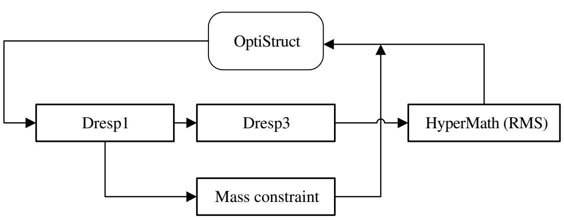

Fig. 9. Data flow of topology optimization in which RMS is taken as the objective function.

Table 2. Initial Structural Sizes of the Lightweight Mirror

Parameter	Value
Diameter	2050 mm
Rib thickness	4.0 mm
Diameter of support hole	170 mm
The front panel thickness	5.0 mm
Mirror thickness	180 mm
Support hole thickness	15.0 mm
Backplane thickness	5.0 mm
Backplane width	30 mm
Total mass	237 kg
Lightweight ratio	88.3%

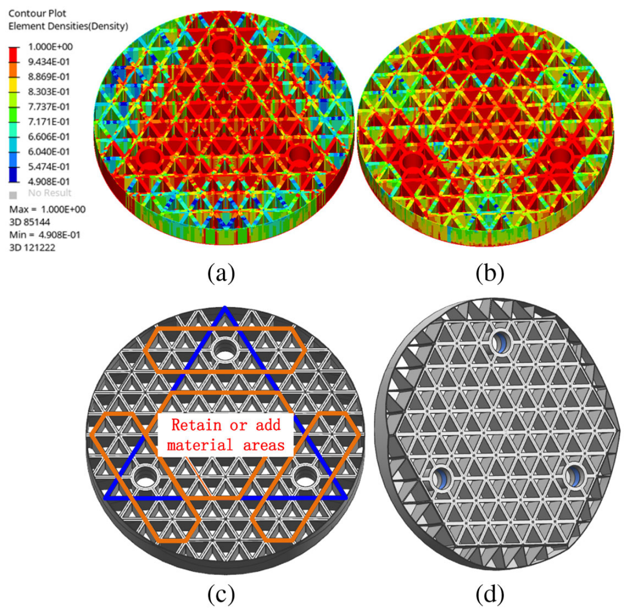

Fig. 10. (a) Material distribution results obtained by first topology optimization in which the surface distortion RMS and the mass are used as the topology objective and the constraint. (b) Material distribution results obtained by second topology optimization in which the eccentricity and the mass are used as the topology objective and the constraint. (c) Marking the area with a solid line in which the material must be retained or added. (d) The 2 m primary mirror obtained by topology optimization.

Table 3. Geometric Parameter of the Lightweight Mirror

Parameter	Value
Diameter	2050 mm
Rib thickness	4/5/6 mm
Diameter of support hole	170 mm
Front panel thickness	5.0 mm
Mirror thickness	180 mm
Support hole thickness	18.0 mm
Backplane thickness	5.0 mm
Backplane width	30 mm
Total mass	233 kg
Lightweight ratio	88.5%

Table 4. Newly Designed Result of Different Design Index

Design Index	Result	Allowed Value
1 g gravity	4.60 nm	5.2 nm
4°C thermal change	1.23 nm	2.0 nm
Forced displacement of 0.1 mm	5.08 nm	5.5 nm
Fundamental frequency	138 Hz	100 Hz

with a density of 1, which means that these elements must be retained or their thicknesses increased. And the blue part represents elements with a density close to zero, requiring material to be either removed or thinned. Therefore, the ribs can be easily grouped based on the topology optimization results. As shown in Fig. 10(c), the fenced area with blue solid line is the area where the material must be retained or added in the first topology optimization. And, the fenced area with the brown solid line is the area where the material must be retained or added in the second topology optimization.

Figure 10(d) is the 3D structure of the 2 m primary mirror, which has combined two topology results. Considering the fabrication and symmetry of the structure, part of the material outside the fenced area is removed. It is undeniable that such structure analysis will lead to the loss of some high-density materials; in other words, the surface accuracy will be lost to some extent. In addition, the thickness of the ribs is increased for the high-density element. Finally, the highly symmetrical mirror structure is obtained, and the geometric parameters and mass characteristics of the mirror are listed in Table 3. Compared to the initial design, the mass of the mirror is reduced by 1.7%.

5. FINITE ELEMENT ANALYSIS

To further prove the advantages of the proposed design method, a flexure support like the one in [12] is adopted. The flexure is shown in Fig. 3(a). To improve the thermal stability, three invar sleeves, which have the same expansion coefficient with SiC material, are bonded to the internal surface of supporting holes using epoxy adhesive (GHJ-01(Z)). The flexure is attached to sleeves and the optical bench by screws, respectively.

The design index of the newly designed primary mirror under different disturbances is analyzed. The analysis results are listed in Table 4. The optimum surface accuracy under gravity with the optical axis horizontal is shown in Fig. 11(a) with the value of RMS as 4.6 nm. As shown in Figs. 11(b) and 11(c), the surface distortion RMS caused by the 4°C temperature change and 0.1 mm assembly error are 1.23 nm and 5.08 nm, respectively. With our method, the lightweight ratio of a 2 m mirror has been improved from 86.8% to 88.5%. Compared to the predesigned primary mirror assembly, the fundamental frequency has increased by 8 Hz.

The sensitivity curves of the predesigned and newly designed 2 m primary mirror are plotted in Fig. 12. Compared to the

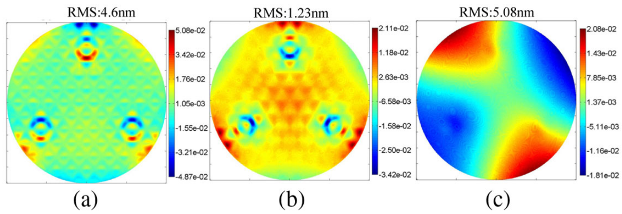

Fig. 11. 2-m reflector mirror obtained by topology optimization.

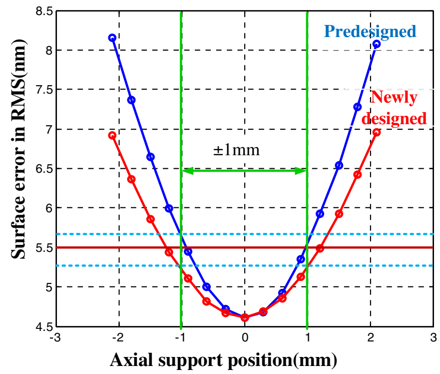

Fig. 12. Trend of distortions depending on axial location of supports, also showing the optimal surface accuracy, flexure accuracy, and gravity surface accuracy index.

sensitivity curve of the predesigned 2 m primary mirror, the sensitivity curve of newly designed has a larger opening size. And the sensitivity to the mount location has been reduced from 1 nm/ ± 1 mm to 0.6 nm/ ± 1 mm. The requirements of various indicators proposed in advance have been satisfied.

6. CONCLUSION

To reduce the sensitivity of a lightweight mirror to the mount location, we introduced the eccentricity of the hyperbola curve. The eccentricity was taken as the objective function in the topology and parametric optimization. With our method, the lightweight ratio of a 2 m mirror has been improved from 86.8% to 88.5%, and the sensitivity to the mount locations has been reduced from 1 nm/ ± 1 mm to 0.6 nm/ ± 1 mm. Compared to the predesigned primary mirror assembly, the fundamental frequency has increased by 8 Hz. The comprehensive performance of the components met the requirements of various indicators proposed in advance. Those results are promising, and show that the eccentricity can reflect the sensitivity to the mount location and the proposed method can effectively reduce the requirement for the assembly accuracy of the mirror support.

Funding. National Natural Science Foundation of China (61705223).

Disclosures. The authors declare no conflicts of interest.

[†]These authors contributed equally to this work.

REFERENCES

1. P. Bely, *The Design and Construction of Large Optical Telescopes* (Springer-Verlag, 2003), pp. 1–28.
2. K. S. Park, S. Y. Chang, and S. K. Youn, "Topology optimization of the primary mirror of a multi-spectral camera," Struct. Multidiscip. Optim. **25**, 46–53 (2003).
3. K. S. Park, J. H. Lee, and S. K. Youn, "Lightweight mirror design method using topology optimization," Opt. Eng. **44**, 053002 (2005).
4. R. Sahu, V. Patel, S. K. Singh, and B. S. Munjal, "Structural optimization of a space mirror to selectively constrain optical aberrations," Struct. Multidiscip. Optim. **55**, 2353–2363 (2017).
5. Y. C. Chen, B. K. Huang, Z. T. You, C. Y. Chan, and T. M. Huang, "Optimization of lightweight structure and supporting bipod flexure for a space mirror," Appl. Opt. **55**, 10382–10391 (2016).
6. S. Liu, R. Hu, Q. Li, P. Zhou, Z. Dong, and R. Kang, "Topology optimization-based lightweight primary mirror design of a large-aperture space telescope," Appl. Opt. **53**, 8318–8325 (2014).
7. G. Liu, L. Guo, X. Wang, and Q. Wu, "Topology and parametric optimization based lightweight design of a space reflective mirror," Opt. Eng. **57**, 075101 (2018).
8. B. Liu, W. Wang, Y. J. Qu, X. P. Li, X. Wang, and H. Zhao, "Design of an adjustable bipod flexure for a large-aperture mirror of a space camera," Appl. Opt. **57**, 4048–4055 (2018).
9. H. Kihm, H. S. Yang, I. K. Moon, J. H. Yeon, S. H. Lee, and Y. W. Lee, "Adjustable bipod flexures for mounting mirrors in a space telescope," Appl. Opt. **51**, 7776–7783 (2012).
10. R. W. Besuner, K. P. Chow, S. E. Kendrick, and S. Streetman, "Selective reinforcement of a 2m-class lightweight mirror for horizontal beam optical testing," Proc. SPIE **7018**, 701816 (2008).
11. P. P. Yoder, *Opto-Mechanical Systems Design* (Taylor & Francis, 2006), pp. 420–421.
12. P. Zhou, S. Xu, C. Yan, and X. Zhang, "Research on neutral surface of lightweight, horizontally supported mirror," Opt. Eng. **57**, 025107 (2018).
13. T. M. Valente and D. Vukobratovich, "A comparison of the merits of open-back, symmetric sandwich, and contoured back mirrors as light-weighted optics," Proc. SPIE **1167**, 20–36 (1989).
14. M. A. Abdulkadyrov, N. M. Vladimirov, N. S. Dobrikov, V. E. Patrikeev, and A. P. Semenov, "Optimizing design and manufacturability of reduced-weight mirrors for astronomy and space applications," J. Opt. Technol. **83**, 168–172 (2016).
15. M. P. Bendsøe and O. Sigmund, "Material interpolation schemes in topology optimization," Arch. Appl. Mech. **69**, 635–654 (1999).
16. S. Amstutz, "Connections between topological sensitivity analysis and material interpolation schemes in topology optimization," Struct. Multidiscip. Optim. **43**, 755–765 (2011).